

## Supplement to

# Observations and Simulations of Meteorological Conditions over Arctic Thick Sea Ice in Late Winter During the Transarktika 2019 Expedition

Günther Heinemann <sup>1,\*</sup>, Sascha Willmes <sup>1</sup>, Lukas Schefczyk <sup>1</sup>, Alexander Makshtas <sup>2</sup>, Vasilii Kustov <sup>2</sup> and Irina Makhotina <sup>2</sup>

<sup>1</sup> Department of Environmental Meteorology, University of Trier, 54286 Trier, Germany; willmes@uni-trier.de (S.W.); schefczyk@uni-trier.de (L.S.)

<sup>2</sup> Arctic and Antarctic Research Institute (AARI), Air–sea interaction department, 199397 St. Petersburg, Russia; maksh@aari.ru (A.M.); kustov@aari.ru (V.K.); i-makhotina@mail.ru (I.M.)

\* Correspondence: heinemann@uni-trier.de; Tel.: +49–651–201–4623

## 1. Changes in CCLM Model Parameterizations

### 1.1. Sea Ice scheme Developments in CCLM

The original sea ice model for CCLM was developed by [1]. The model used the approach of [2] applied to a two–layer sea–ice model. For thin ice, only one layer of ice without snow is assumed to be present. For thick ice, a snow layer of a fixed depth was assumed to be on top of the ice layer. In both cases, the energy budget (and as a result the surface temperature) was calculated only for the upper layer. In the case of thick ice, the temperature at the snow/ice interface was initialized using the forcing data (e.g. reanalyses), but was then kept constant. As a consequence, surface temperature variations resulted completely from the energy budget of the snow layer. Sea ice albedo had a constant value of 0.7 in [1]. The albedo parameterization was improved by [3], who used the scheme of [4]. The albedo using this scheme depends on ice thickness and temperature and includes also a parameterization of melt ponds. There was no penetration of solar radiation through the snow or ice layers. The different parameterizations are summarized in Table S1, where the state of [3] is referred to as “old” scheme.

**Table S1.** Sea ice and parameterizations in CCLM as used in the “old” version [3] and in the present paper (“new”).

Sea Ice Physics	Old	New	References
Thin ice	No snow layer	No snow layer	[1]
Thick ice	Fixed snow layer 0.1m	Variable snow layer	
Penetration of solar radiation	–	In snow and ice layer	[5]
Temperature gradients	Linear	Non–linear depending on layer thickness	[2]
Heat budgets	Thick ice: only in snow layer	Snow and ice layer	
Albedo	Modified Køltzow scheme	Modified Køltzow scheme	[4]

For the present study, further improvements of the sea ice scheme were implemented (Table S1). A variable height of the snow layer was introduced by assuming a snow layer thickness of 10% of the sea–ice thickness. This seems to be a reasonable assumption, since recent snow depth retrievals [6] showed mean snow depths between 5 cm and 20 cm depending on the season. Coupled heat budgets of the snow and ice layers are now calculated, and it is accounted for the penetration of solar radiation through the snow and ice layers. While conductive heat fluxes were computed assuming linear temperature profiles

in the old version, a variable non-linear shape of the temperature profiles according to [2] is now used as a function of the layer thickness.

### 1.2. Tile Approach Developments in CCLM

The tile approach is a standard method in RCMs to consider sub-grid scale inhomogeneities in the flux calculation within a grid cell [7]. In its application to fractional sea ice cover, sea ice is considered as a mean concentration over a model grid box, and surface fluxes are computed separately for the water and ice fractions. The grid scale flux is then calculated as the average of water and ice fluxes weighted with their fractions. Most uncoupled RCMs assume a fixed thick ice thickness (e.g. 1 m) for the ice fraction and open water for the water fraction. The latter is unrealistic during winter, where leads and polynyas are almost totally covered with thin ice [8]. The thin-ice coverage has a large effect on the surface fluxes and sea ice production [9] [3]. As a consequence, [3] introduced a tile approach for sea ice in CCLM, which uses separate grid-scale and sub-grid scale ice thicknesses. This parameterization was different for  $SIC \leq 0.7$  (typical for polynyas) and for large ice concentration ( $SIC > 0.7$ ). Both ice thicknesses were prescribed, [3] and [10] recommend for polynyas 30 cm for the grid-scale and 1 cm for the sub-grid scale ice thickness. Outside polynyas ( $SIC > 70\%$ ) the grid-scale ice thickness was that of PIOMAS, and sub-grid scale ice thickness was taken as 1 cm (Table S2).

**Table S2.** Tile approach parameterizations in CCLM as used in the “old” version [3] and in the present paper (“new”).

Ice Thickness	Old	New	References
General: preset value	PIOMAS, subgrid-scale ice thickness for missing PIOMAS data and $SIC > 0$	PIOMAS, depending on SIC for missing PIOMAS data	[11]
Subgrid-scale ice thickness	Fixed value (1 cm)	Variable, computed from thermodynamic ice growth	
Grid-scale ice thickness	$SIC > 0.7$ : preset value $SIC \leq 0.7$ : 30 cm	$SIC > 0.7$ : preset value $SIC \leq 0.7$ : depending on temperature and SIC	
<b>Averaging</b>			
Averaging of heat fluxes	Linear with SIC	Linear with SIC	
Averaging of transfer coefficients	Linear with SIC	Non-linear: form drag for momentum, effective coefficients for heat	[12]

For the present study, further modifications of the tile approach were implemented (Table S2). Since PIOMAS ice thicknesses are not always consistent with the SIC from satellite data (particularly for polynyas and in the marginal ice zone), these grid points have to be attributed to a grid-scale ice thickness, which is a function of SIC in the new version. This avoids thin-ice areas in the marginal ice zone. For polynyas, the grid-scale thickness was made variable as a function of temperature and SIC. In a first step, an intermediate grid-scale thickness is computed, which is the preset (PIOMAS) value at the melting point and the thickness by thermodynamic growth (see below) below  $-10^\circ\text{C}$ . This accounts for the fact that during winter new ice is formed in polynyas, which contributes to the ice thickness, while during summer all ice in polynyas is considered as thick ice with open water for the non-ice fraction. The final grid-scale thickness is then computed as a linear function of SIC assuming a value of zero for  $SIC \leq 0.15$ , taking the intermediate thickness for  $SIC = 0.3$  and the preset value for  $SIC > 0.7$ . For the sub-grid scale fraction, the ice thickness is now computed by a bulk estimation of the thermodynamic growth for a prescribed time period, which is 24 h for polynyas and 6 h for leads. The sub-grid scale ice thickness is set to zero for  $SIC \leq 0.15$ , which results that open water is assumed for  $SIC \leq 0.15$ . This results in realistic thin ice values when compared to the polynya study of [13].

While the averaging for the surface heat fluxes is the same for both versions, the averaging for the momentum flux and transfer coefficients was modified in the new version. For the transfer coefficient for momentum (drag coefficient), the form drag parameterization of [12] was implemented. A further modification was made for the averaging of transfer coefficients for heat. Since a bulk approach [14] is used for the calculation of turbulent fluxes at the ice and thin-ice/water surfaces, a recalculation of averaged transfer coefficients from averaged gradients as done e.g. in [15] can lead to inconsistent results. Thus, effective coefficients for heat are calculated using the averaged fluxes and averaged gradients. The second reason for effective coefficients for heat is that CCLM uses only transfer coefficients and diffusion coefficients for the exchange between different program modules. In order to enable that the tile approach for fluxes is adequately considered for the computation of tendencies in the boundary layer, the use of effective coefficients for heat is necessary.

### 1.3. Changes for the Boundary Layer Parameterization in CCLM

The parameterization of turbulence in the stable boundary layer (SBL) was adapted to [16], who used a lower limit of minimum diffusion coefficients to improve the simulation of the surface inversion for weak wind conditions over the Antarctic plateau (Table S3). An improvement was found also for the katabatic wind structure over Greenland [17]. The diffusion coefficients affect the computation of the turbulent kinetic energy (TKE), where CCLM uses a prognostic TKE scheme (1.5 order turbulence closure at level 2.5, [18]), see [19] for a full description. In addition, CCLM uses a parameterization for the generation of TKE by sub-grid eddies via a thermal circulation term in the TKE equation [20], which increases the TKE production particularly in the SBL. This term is controlled by an inhomogeneity length scale, which has a standard value of 500 m. [21] use CCLM for the Antarctic with a minimal value of 0.03 m<sup>2</sup>/s and set the thermal circulation length scale to 10 m. [16] and [17] neglect the thermal circulation term completely (as in [20]). In the present paper, we also neglect the thermal circulation term. A further modification was introduced for the asymptotic mixing length in the SBL. While in the old version this length is described with a fixed value of 500 m, we use a more realistic parameterization depending on TKE and stability as introduced by [22]. Here the local buoyancy length is used for limiting the mixing length in the SBL. The experimental study of [23] shows that the local buoyancy length is suitable for the turbulence parameterization in the SBL.

Roughness lengths for ocean are calculated using the parameterization of [24] in the old and new version (Table S3). While previously a fixed value of 1 mm was used for the roughness lengths of momentum ( $z_0$ ) and heat ( $z_T$ ), we now use  $z_0$  as a function of the ice thickness [25] being 0.4 mm for young ice (ice thickness less than 0.4 m) and 4 cm for closed pack ice with ridges (ice thickness more than 3 m). The roughness length for heat is parameterized according to [26] with the limitations that the maximum value of  $z_T/z_0$  is 1, and the minimum is  $0.5 \times 10^{-4}$ , which agrees with the values given by [25] for thick ice.

**Table S3.** Boundary layer parameterizations in CCLM as used in the “old” version [3] with the adaption of the minimum diffusion coefficients and sub-grid TKE production of [16,17] (original values shown in brackets), and as used in the present paper (“new”).

Roughness lengths	Old	New	References
Ocean	Modified Charnock relation	Modified Charnock relation	[24]
Sea ice	Fixed value (1 mm)	Momentum: $z_0$ dependent on ice thickness; heat: ratio $z_T/z_0$ dependent on roughness Reynolds number	[25], [26]
<b>SBL</b>			
Minimum diffusion coefficients	0.01 m <sup>2</sup> /s (0.4 m <sup>2</sup> /s)	0.01 m <sup>2</sup> /s	[16], [17]

Asymptotic mixing length	500 m	Depending on TKE and stability	[22]
Parameter (pat_len) for TKE production from sub-grid thermal circulation	0 m (500 m)	0 m	[16], [17]

Figure S1 shows comparisons between different parameterizations and observations for the 2m-temperature and 10m-wind speed. Old-defurb (red symbols) is the run with the old version using the original values for the SBL parameterization (Table S3). The bias is slightly larger (more negative) than for the new version (black symbols), the RMSE is about 1.5 K higher. The introduction of the new SBL parameterization (reduction of minimum diffusion coefficients and the neglect of TKE-production by sub-grid eddies, old\_newturb) was found to largely improve the simulation of the SBL over the Greenland [17], ice sheet and over Antarctica [16]. The comparison for Transarktika shows an increase of the negative bias of about 1.5K compared to the old-defurb run, the RMSE is increased by about the same value. The new version shows the smallest values for bias and RMSE for the temperature. The run "new\_linear" (green symbols) is the new version but with linear averaging of surface fluxes and transfer coefficients (Table S2). It shows slightly larger values of bias and RMSE for temperature than the new version. For the wind speed, all parameterizations show the same RMSE. The bias is close to zero, except for the new version, where the bias is about 1 m/s. This leads to the conclusion that the main impact is given by the new parameterization of the roughness length and the drag coefficient in the new version. For the simulation of the average daily temperature amplitude, the new and the new-linear run are both very close to the observations, while the old runs largely overestimate the temperature amplitude. This is caused by the underestimation of the temperature during periods with low cloudiness.

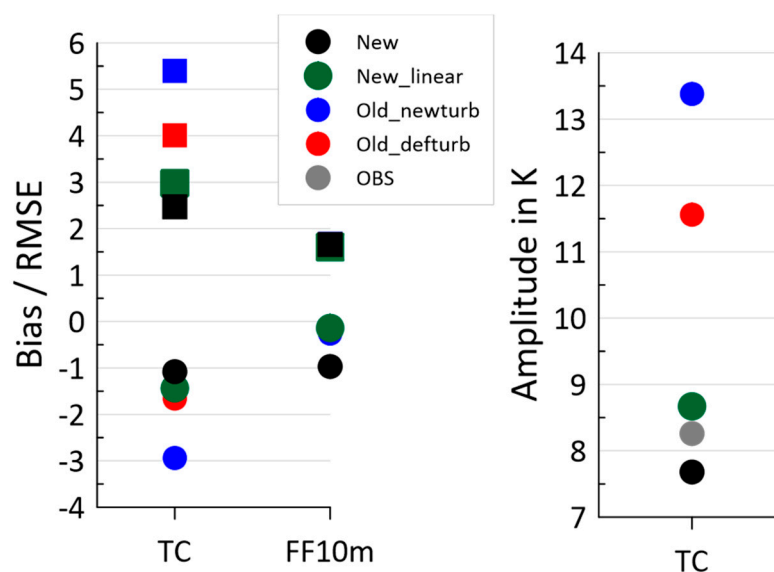


**Figure S1.** left: Bias (dots) and RMSE (squares) for the 2m-temperature (TC, values in K) and the 10m-wind. (FF10m, values in m/s) for different parameterizations (see text). Right: average daily 2m-temperature amplitude (in K) of observations and for different parameterizations.

## References

- Schröder, D.; Heinemann, G.; Willmes, S. The impact of a thermodynamic sea-ice module in the COSMO numerical weather prediction model on simulations for the Laptev Sea, Siberian Arctic. *Polar Research* **2011**, *30*, 6334, doi:10.3402/polar.v30i0.6334.
- Mironov, D.; Ritter, B.; Schulz, J.-P.; Buchhold, M.; Lange, M.; MacHulskaya, E. Parameterisation of sea and lake ice in numerical weather prediction models of the German Weather Service. *Tellus A: Dynamic Meteorology and Oceanography* **2012**, *64*, 17330, doi:10.3402/tellusa.v64i0.17330.

3. Gutjahr, O.; Heinemann, G.; Preußner, A.; Willmes, S.; Drüe, C. Quantification of ice production in Laptev Sea polynyas and its sensitivity to thin-ice parameterizations in a regional climate model. *The Cryosphere* **2016**, *10*, 2999–3019, doi:10.5194/tc-10-2999-2016.
4. Køltzow, M. The effect of a new snow and sea ice albedo scheme on regional climate model simulations. *J. Geophys. Res.* **2007**, *112*, doi:10.1029/2006JD007693.
5. Perovich, D.K. Light reflection and transmission by a temperate snow cover. *J. Glaciol.* **2007**, *53*, 201–210, doi:10.3189/172756507782202919.
6. Zhang, C.; Ji, Q.; Pang, X.; Su, J.; Liu, C. Comparison of passive microwave remote-sensing snow-depth products on Arctic sea ice. *Polar Research* **2019**, *38*, doi:10.33265/polar.v38.3432.
7. Heinemann, G.; Kerschgens, M. Simulation of surface energy fluxes using high-resolution non-hydrostatic simulations and comparisons with measurements for the LITFASS-2003 experiment. *Boundary-Layer Meteorol* **2006**, *121*, 195–220, doi:10.1007/s10546-006-9107-z.
8. Preußner, A.; Ohshima, K.I.; Iwamoto, K.; Willmes, S.; Heinemann, G. Retrieval of Wintertime Sea Ice Production in Arctic Polynyas Using Thermal Infrared and Passive Microwave Remote Sensing Data. *J. Geophys. Res. Oceans* **2019**, *124*, 5503–5528, doi:10.1029/2019JC014976.
9. Bauer, M.; Schröder, D.; Heinemann, G.; Willmes, S.; Ebner, L. Quantifying polynya ice production in the Laptev Sea with the COSMO model. *Polar Research* **2013**, *32*, 20922, doi:10.3402/polar.v32i0.20922.
10. Gutjahr, O.; Heinemann, G. A model-based comparison of extreme winds in the Arctic and around Greenland. *Int. J. Climatol.* **2018**, *38*, 5272–5292, doi:10.1002/joc.5729.
11. Zhang, J.; Rothrock, D.A. Modeling Global Sea Ice with a Thickness and Enthalpy Distribution Model in Generalized Curvilinear Coordinates. *Mon. Wea. Rev.* **2003**, *131*, 845–861, doi:10.1175/1520-0493(2003)131<0845:MGSIIWA>2.0.CO;2.
12. Lüpkes, C.; Gryanik, V.M. A stability-dependent parametrization of transfer coefficients for momentum and heat over polar sea ice to be used in climate models. *J. Geophys. Res.* **2015**, *120*, 552–581, doi:10.1002/2014JD022418.
13. Willmes, S.; Krumpen, T.; Adams, S.; Rabenstein, L.; Haas, C.; Hoelemann, J.; Hendricks, S.; Heinemann, G. Cross-validation of polynya monitoring methods from multisensor satellite and airborne data: a case study for the Laptev Sea. *Canadian Journal of Remote Sensing* **2010**, *36*, S196–S210, doi:10.5589/m10-012.
14. Louis, J.-F. A parametric model of vertical eddy fluxes in the atmosphere. *Boundary-Layer Meteorology* **1979**, *17*, 187–202, doi:10.1007/BF00117978.
15. Sedlar, J.; Tjernström, M.; Rinke, A.; Orr, A.; Cassano, J.; Fettweis, X.; Heinemann, G.; Seefeldt, M.; Solomon, A.; Matthes, H.; et al. Confronting Arctic troposphere, clouds, and surface energy budget representations in regional climate models with observations. *J. Geophys. Res.* **2020**, doi:10.1029/2019JD031783.
16. Zentek, R.; Heinemann, G. Verification of the regional atmospheric model CCLM v5.0 with conventional data and lidar measurements in Antarctica. *Geosci. Model Dev.* **2020**, *13*, 1809–1825, doi:10.5194/gmd-13-1809-2020.
17. Heinemann, G. Assessment of Regional Climate Model Simulations of the Katabatic Boundary Layer Structure over Greenland. *Atmosphere* **2020**, *11*, 571, doi:10.3390/atmos11060571.
18. Mellor, G.L.; Yamada, T. A Hierarchy of Turbulence Closure Models for Planetary Boundary Layers. *J. Atmos. Sci.* **1974**, *31*, 1791–1806, doi:10.1175/1520-0469(1974)031<1791:AHOTCM>2.0.CO;2.
19. Zentek, R. COSMO documentation (archived version from 2019, uploaded with permission of the DWD), 2019. <https://zenodo.org/record/3339384> (accessed on 13 May 2020).
20. Cerenzia, I.; Tampieri, F.; Tesini, S. Diagnosis of Turbulence Schema in Stable Atmospheric Conditions and Sensitivity Tests. *COSMO Newsletter*, 2014.
21. Souverijns, N.; Gossart, A.; Demuzere, M.; Lenaerts, J.T.M.; Medley, B.; Gorodetskaya, I.V.; Vanden Broucke, S.; van Lipzig, N.P.M. A New Regional Climate Model for POLAR-CORDEX: Evaluation of a 30-Year Hindcast with COSMO-CLM 2 Over Antarctica. *J. Geophys. Res.* **2019**, *124*, 1405–1427, doi:10.1029/2018JD028862.
22. Hebbinghaus, H.; Heinemann, G. LM simulations of the Greenland boundary layer, comparison with local measurements and SNOWPACK simulations of drifting snow. *Cold Regions Science and Technology* **2006**, *46*, 36–51, doi:10.1016/j.coldregions.2006.05.003.
23. Heinemann, G. Local Similarity Properties of the Continuously Turbulent Stable Boundary Layer over Greenland. *Boundary-Layer Meteorol* **2004**, *112*, 283–305, doi:10.1023/B:BOUN.0000027908.19080.b7.
24. Charnock, H. Wind stress on a water surface. *Q.J.R. Meteorol. Soc.* **1955**, *81*, 639–640, doi:10.1002/qj.49708135027.
25. Weiss, A.I.; King, J.; Lachlan-Cope, T.; Ladkin, R. On the effective aerodynamic and scalar roughness length of Weddell Sea ice. *J. Geophys. Res.* **2011**, *116*, doi:10.1029/2011JD015949.
26. Andreas, E.L. A theory for the scalar roughness and the scalar transfer coefficients over snow and sea ice. *Boundary-Layer Meteorol* **1987**, *38*, 159–184, doi:10.1007/BF00121562.